The structure of barium in the hexagonal close-packed phase under high pressure

1997 J. Phys.: Condens. Matter 9 3489

(http://iopscience.iop.org/0953-8984/9/17/001)

J. Phys.: Condens. Matter **9** (1997) 3489–3502. Printed in the UK PII: S0953-8984(97)79152-5

The structure of barium in the hexagonal close-packed phase under high pressure

W-S Zeng†§, V Heine‡ and O Jepsen†

† Max-Planck-Institut für Festkörperforschung, Heisenbergstrasse 1, D-70569 Stuttgart, Germany
‡ Cavendish Laboratory, University of Cambridge, Madingley Road, Cambridge CB3 0HE, UK

Received 1 November 1996

Abstract. Recent experimental results on two hcp phases of barium under high pressure show interesting variation of the lattice parameters. They are here interpreted in terms of electronic structure calculations by using the linear muffin-tin orbital method and generalized pseudopotential theory with a nearly-free-electron plus tight-binding-bond approach. In phase II (5.5–12.6 GPa) the dramatic drop in *c/a* is an instability analogous to that in the group II metals Mg to Hg but with the transfer of s to d electrons playing a crucial role in Ba. Meanwhile in phase V (45–90 GPa), the instability decreases a lot due to the core repulsion at very high pressure. The *c/a* ratio in phase V is somewhat less than the expected ideal value due to some admixture of 5d and 4f components in the wave function.

1. Introduction

The understanding of the physical properties of the heavy alkaline-earth metals has increased significantly with the help of electronic structure calculations and the use of experimental techniques especially at high pressure. The d bands in close proximity to the Fermi level and some electronic transfers (e.g. s to p and d, etc) are considered as the main reason for the 'abnormal' physical properties. At atmospheric pressure barium has a body-centred-cubic (bcc) structure and the bottom of the 5d band has crossed below the Fermi level [1]. Besides the sp–d hybridization, the substantial filling of the 5d bands is also very important for the physical properties of barium [2–4]. The filling of the 5d band can be increased by the application of high pressure. Under high pressure, an s–d electronic transfer may occur due to the crossover of the 6s and 5d bands. The following high-pressure investigations on barium attracted our attention, and the purpose of the present work is to see whether the s–d electronic transfer induced by pressure will play an important role and how strong it is.

Takemura [5], by using high pressure (up to 90 GPa) and powder x-ray-diffraction (XRD) techniques, reported that barium at room temperature has *two* hcp (hexagonal close-packed) phases under pressure with the following interesting features: (a) the *c/a* ratio of phase II (in the pressure range: 5.5–12.6 GPa) decreases dramatically with pressure, and (b) the *c/a* ratio of phase V (in the pressure range: 45–90 GPa) is almost pressure independent with a value of 1.575, which is fairly close to $\sqrt{8/3} \approx 1.632$, the value of the ideal hcp structure but yet significantly less. As a summary, we show their experimental data in figure 1. A few elements are found to transform back to the same crystal structure under

§ Present address: Center for Optoelectronics and Imaging, and Department of Electrical Engineering, University of Rochester, 240 East River Road, Rochester, NY 14623, USA.

0953-8984/97/173489+14$19.50

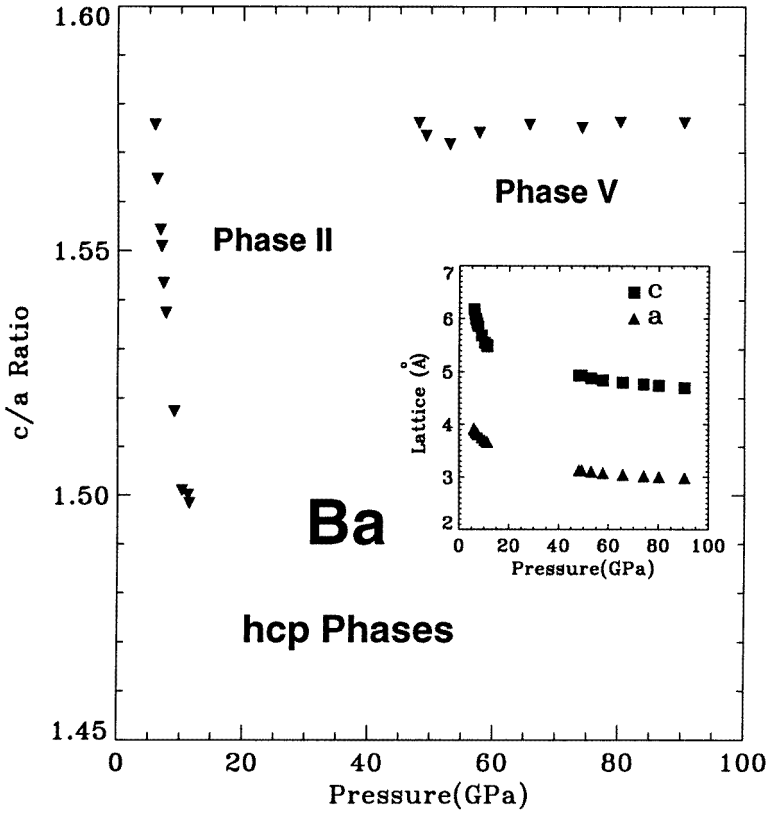

Figure 1. The experimental structure data for barium under high pressure. The lattice constants *a* and *c* are shown in the inset.

pressure. They are La with fcc → distorted fcc → fcc isostructural transitions [6, 7], and Cs [8–10] and Ce [11, 12] with fcc → fcc isostructural transitions. The origins of these transitions are quite different from each other (see reference [7–12]). The different variation of the *c/a* ratios as a function of pressure should indicate different stabilizing mechanisms in the two hcp phases of barium.

In this paper, we will interpret the above two interesting features in terms of electronic structure calculations. A linear muffin-tin orbital (LMTO) calculation in the atomic-sphere approximation (ASA) [13, 14] was performed firstly to obtain the occupation numbers of s, p, d and f orbitals as functions of pressure in the hcp structure of barium. The electronic transfers can be seen clearly from our LMTO-ASA calculation. The increasing d character in place of s and p character favours a short bonding length. However, this argument cannot explain the above two features since both lattice constants *a* and *c* in the hcp structure become shorter with increasing pressure, as shown in the inset of figure 1. Thus we have to use the full-potential LMTO (FP-LMTO) [15, 16] method to find the relation between the *c/a* ratio and the total energy of the system. In particular, we have performed some model calculations with different orbitals eliminated from the basis set to investigate their importance. In order to give a good physical explanation of the two interesting features mentioned above, we have used a generalized pseudopotential theory (GPT) [17] with a nearly-free-electron plus tight-binding-bond (NFE-TBB) [18–20] approach in real space to

find a relationship between instability and the variation of the *c/a* ratio. The d-electron component is found to be the main driving force for the variation of the *c/a* ratio in phase II. At very high pressure (e.g. in phase V), the 'hard-sphere' nature of the atoms plays the dominant role.

Pseudopotential theory has been used previously to discuss the large variation of the *c/a* ratio in the series of Be, Mg, Zn, Cd and Hg, both from the real-space and reciprocal-space points of view [21–24]. The rapid variation of *c/a* in this series can be described as a developing instability. This is caused by a systematic trend in the pseudopotential associated with decreasing sp hybridization in the series as seen in the variation of q_0, the position of the first zero of the pseudopotential in reciprocal space, and an explanation of the variation of the *c/a* ratio in the hcp structure from Be to Cd can be developed. The variation of q_0 can in turn be related to atomic properties such as the radius of the ion core and the sp promotion energy [25]. In barium, because of the substantial filling of the 5d band as seen from self-consistent LMTO calculations [2–4], the mechanism of the large variation of the *c/a* ratio is expected to be different. We will show that for barium in phase II the rapid decrease of the *c/a* ratio with pressure is a result of a similar instability but driven by the transfer of s to d electrons.

Other 'good' hcp metals have *c/a* ratios closer to the ideal value. We may expect barium to approach a 'hard-sphere' behaviour under very high pressure (i.e. in phase V) as all materials tend to. Although increased d character will lead to an additional attractive interaction between atoms, the repulsion between atoms at very small interatomic distance corresponding to very high pressure becomes much more important. This will overwhelm the instability apparent in phase II and then create a new stability at a larger *c/a* ratio closer to the ideal value. We will discuss this in detail in section 4.

The paper is organized as follows. Section 2 will describe briefly the calculational methods and some parameters used in this paper. In section 3 we will show the results of our LMTO calculation with some discussion. The instability in phase II and the changes of this instability in phase V will be discussed in section 4. The conclusions are given in section 5.

2. Details of the calculational methods

In this section, we will briefly describe the calculational methods used in this paper.

We performed self-consistent density functional [26, 27] calculations using two versions of the LMTO method [13]. The tight-binding LMTO-ASA version [28] was used to study the changes of the orbital occupations as a function of pressure. This method has been described in detail elsewhere [29, 30] and a recent detailed application has been published by Jepsen and Andersen [14]. In this method, the one-electron Schrödinger equation with a local exchange–correlation potential [31] is solved self-consistently in scalar-relativistic form, i.e. all relativistic effects are included except the spin–orbit coupling. The space is divided into muffin-tin spheres centred at each atom, plus the remaining interstitial region. The basis functions in the spheres are constructed from radial Schrödinger equation solutions and their energy derivatives at some set of energies ε_ν, in the middle of the energy ranges of interest. In the interstitial region, the basis functions are solutions of the Helmholtz equation: $(\nabla^2 + \varepsilon) f(r, \varepsilon) = 0$ with some fixed value of the average kinetic energy $\varepsilon = \kappa_\nu^2$, called 'LMTO envelopes'. In the LMTO-ASA calculation, the interstitial region is effectively eliminated and only one LMTO envelope per lm with $\kappa_\nu^2 = 0$ is included. We use the orbital projection technique to get the occupation number of each orbital, projecting the charge onto the l (l = s, p, d and f) orbitals and then calculating the projected density of

states (DOS) $N_l(E)$. The corresponding occupation number n_l of the l-orbital can thus be calculated [14]:

$$n_l = \int^{E_F} N_l(E)\ \mathrm{d}E. \tag{1}$$

We used a large number of $\boldsymbol{k}$-points and the tetrahedron method [32] for all $\boldsymbol{k}$-space integrations.

In order to obtain an accurate total energy of the system, the potential has to be considered properly, not as a muffin-tin average but constructed self-consistently from the wave functions [13]. For this purpose the FP-LMTO method was used with a so-called triple-κ basis set [15, 16] with $\kappa_1^2 = 0, \kappa_2^2 = -1$ and $\kappa_3^2 = -2.3$ Ryd to give a very complete basis set and avoid any geometrical approximation of the potential. The muffin-tin spheres were non-overlapping and we treated the 6s, 5p, 5d, 4f as valence states. By removing some orbitals (especially 5d and 4f) from the basis set we can investigate their importance. We found that for phase V the whole of the triple-κ basis must be included for satisfactory convergence, while for phase II a double-κ basis was found more or less sufficient though the calculated *c/a* ratio is somewhat larger than the observed value. This is consistent with other total energy calculations with the FP-LMTO method for other elements [33–35].

For the generalized pseudopotential theory (GPT) calculations, the pair potential of barium is calculated with the nearly-free-electron tight-binding-bond (NFE-TBB) method [18–20] to show the instability in *c/a*. It is not sufficient to use the simple pseudopotential theory of reference [21–24] because of the strong d component as discussed by Jank and Hafner [36]. The purpose of this part of the work was to give a simple semiquantitative interpretation of the experimental results, not to reproduce them by accurate calculation. Thus the pair potential was not recalculated at each volume since it is slowly varying with electron density [22], and we simply use the pair potential from reference [36], unchanged, including both their sp- and d-electron contributions. The distortion compared with the ideal hcp structure is studied by calculating the energy of the system and as a function of the *c/a* ratio at constant volume, at various volumes corresponding to various pressures in the range covered by the experimental measurements.

3. LMTO results for phases II and V

In this section, we will show our LMTO-ASA and FP-LMTO calculational results and some discussions.

Figure 2 shows the calculated occupation numbers of the s, p, d, and f states as a function of the pressure as calculated with the LMTO-ASA method. The only input parameters in the LMTO-ASA calculations were the lattice constants as shown in the inset of figure 1. Clearly, the electronic transfer from s to d in barium distinguishes it from the series Mg to Hg [21]. There is clearly a strong transfer from the s and p orbitals into d orbitals with a small transfer into f in phase II. Additionally in the phase transition from phase II to phase V there is a larger transfer from s to f, and then a very small transfer from d to f with increasing pressure in phase V. However, the dominant effect is an s-to-d electronic transition induced by pressure all within the same hcp structure of barium. The main feature of the density of states for barium under ambient conditions is that the bottom of the 5d band dips below the Fermi level [1]. Thus the electronic structure contains a substantial filling of the 5d bands, as well as the hybridization of the 5d states into the 6s, 6p bands [2–4]. Under pressure the energy of the lowest 5d band falls further below the Fermi level,

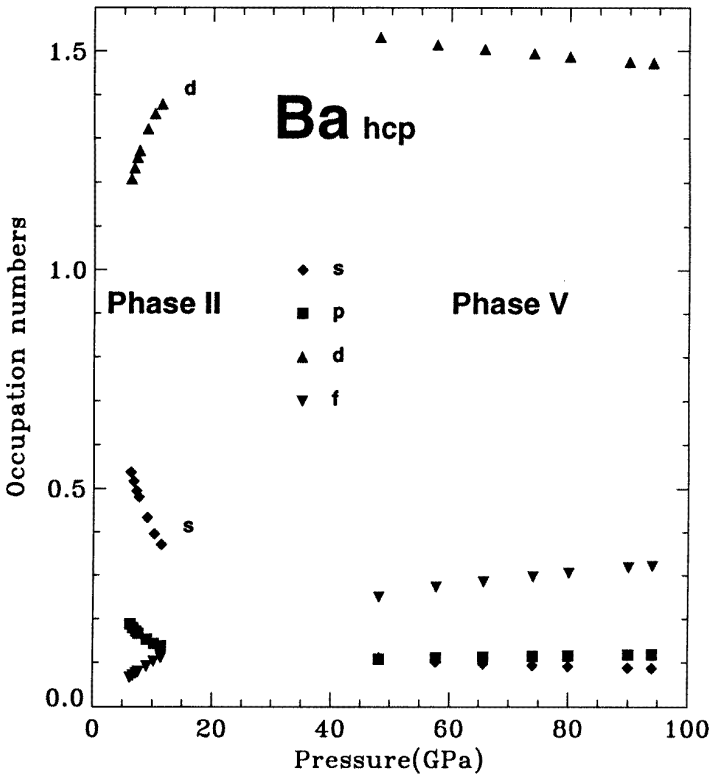

Figure 2. The LMTO-ASA calculated occupation numbers of s, p, d, and f orbitals as functions of pressure.

even to below the bottom of the 6s band, due to increasing broadening of the 5d band and a drop in its centre of gravity. At the same time the 6s band rises due to the increase in kinetic energy and being squeezed into the repulsive core, thus contributing to the 6s-to-5d electron transfer. This s-to-d transfer under pressure in the alkaline-earth metals has been known of for a long time [2–4] and is also evident in our calculation (figure 2). It is a fingerprint of the fcc-to-bcc phase transition in several alkaline-earth metals [37–38], and indeed can be noted in other elements [2–4, 40]. The 5d orbitals are favoured relative to the 6s6p at smaller interatomic spacings under pressure, and conversely the 5d orbitals favour shorter bond lengths. However, this argument cannot explain the dramatic drop in the *c/a* ratio in phase II since a change of *c/a* from the ideal value increases six bond lengths while reducing six others to the twelve nearest neighbours at constant volume or pressure. Thus the explanation for the drop in *c/a* in phase II (figure 1) cannot be found in the number of d electrons alone as determined from the LMTO-ASA calculations of figure 2: it is necessary to go to the FP-LMTO method for full calculation of the total energy as a function of *c/a*. Under very high pressure in phase V, the occupied number of s states is very small ($\simeq$0.1/atom) and the s band is effectively emptied as shown in figure 2. Then the physical properties will be dominated by the repulsion of the 5p core and incomplete screening of the $z = 2$ ionic charges as discussed later.

In figure 3 we show our FP-LMTO results for the total energy as a function of *c/a* ratio at constant volume chosen to correspond to some of the measured pressures. For these

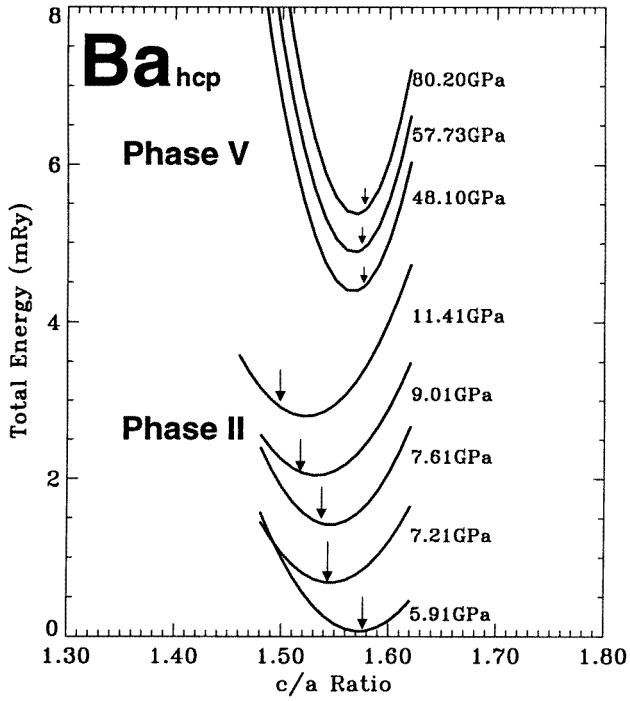

Figure 3. The total energy (relative) of barium in the hcp structure in phases II and V as a function of the *c/a* ratio, calculated with the FP-LMTO method with a large basis set. Each curve is displaced vertically by an arbitrary amount for clarity. The arrows indicate the *c/a* ratios found experimentally.

results we used a large basis set to ensure completeness: three s orbitals, three radial p orbitals, two radial d orbitals and one radial f orbital. The curves in figure 3 are displaced vertically by arbitrary amounts for clarity. The arrows indicate the experimental *c/a* ratios, which are seen to agree quite well with the calculated energy minima. Recently, various other FP-LMTO calculations on the total energy of some elements have agreed very well with experimental observations, indicating that the FP-LMTO method is a good and fast calculational method. For example, the structural sequence bcc $\rightarrow$ hcp $\rightarrow$ fcc $\rightarrow$ bcc for Cr and Mo and bcc $\rightarrow$ hcp $\rightarrow$ fcc for W as a function of pressure were obtained correctly [33], as were the *c/a* ratios in the hcp structure of Ti, Zr and Hf at ambient condition [34]. Similarly, the total energies and bonding features determining the crystallographic structures have been studied in titanium–carbon and tungsten–carbon systems [35], the theoretical investigations comparing fairly well with experiment.

At low pressure in phase II (e.g. 5.91 GPa), the calculated *c/a* ratio is very close to the observed value. As the pressure is increased, the minimum position of the total energy is found to shift rapidly to lower *c/a* ratio. This corresponds to a developing instability in phase II and will be discussed in section 4. In phase V, the total energy increases steeply with decreasing volume, more than its variation with *c/a* whose equilibrium value remains nearly constant a bit below the ideal value both in experiment and in the calculated results. The calculated energy can be fitted quite well by a simple formula

$$E_{tot} = A(V)((c/a) - (c/a)_{exp})^2 + B(V) \tag{2}$$

where $A(V)$ and $B(V)$ both increase with decreasing volume. The curves of phase V in figure 3 are much steeper than those of phase II, indicating that the $A(V)$ term in phase V is much larger than that of phase II. The physical reason for this is that, although the s–d transfer is in the direction of lowering the total energy, the repulsion of the core, the squeezing of the conduction electrons into the core and the incomplete screening of the ionic charge all contribute to a hard-sphere type of behaviour at very small interatomic distance, as will be discussed later.

In order to elucidate the above-described phenomena further, we will perform a number of model calculations or hypothetical computer experiments which focus on the effects of each orbital. Similar calculations were reported by Ahuja *et al* on calcium under high pressure [41]. These calculations will provide us with a detailed analysis of what features of the electronic structure determine the structural characteristics in hcp barium under pressure. The mechanisms for the drop in *c/a* ratio in phase II and almost constant *c/a* ratio in phase V will be found to be different. Our results are shown in figure 4(a) (pressure = 7.21 GPa), typical for phase II, and figure 4(b) (pressure = 57.73 GPa), typical for phase V. As in figure 3, each curve is displaced vertically by an arbitrary amount for clarity. The total energy of the system is shown using different basis sets for the valence states, as a function of the *c/a* ratio at a constant volume corresponding to the experimental volume.

For phase II we first included in the basis set only s and p orbitals as shown by the top curve in figure 4(a). The label 2s2p means that only s and p orbitals were included in the valence states, two separate radial s and p orbitals corresponding to two energies ε_ν each. The second curve labelled 3s3p, with a larger basis set but still without d orbitals, is almost parallel to the first, so we may consider our results converged, within the stated restriction of course. Note that the minimum is at *c/a* larger than the ideal value (1.632) as it is in Zn and Cd with predominantly sp electrons. The other curves in figure 4(a) show that adding one radial d orbital inside the muffin-tin sphere reduces *c/a* to 1.59, i.e. less than for the ideal structure, and two such d orbitals reduce it further to the experimental value of 1.54 at 7.21 GPa. The inclusion of f orbitals inside and outside the spheres does not affect the results significantly.

Similar calculations for phase V are shown in figure 4(b). Again the exclusion of d orbitals in the basis set results in *c/a* being larger than the ideal value, and the inclusion of two radial d orbitals brings it down to the measured value 1.57, less than the ideal value. However, in each case the value of *c/a* is closer to the ideal value than in figure 4(a), indicating a 'hard-sphere' type of situation as might be expected at such high pressure.

4. The behaviour of *c/a* in phases II and V

In this section, we will consider the instability of the *c/a* ratio in phase II and the short-range repulsion in phase V.

This instability can best be understood in terms of pseudopotentials and second-order perturbation theory. This was used to explain the instability in the series Be to Hg [21–24] and we will take it over to apply to barium with one modification. In this theory, the total energy of the system for arbitrary position R_{ij} of the atoms can be written as [23, 19]

$$E_{tot} = f(V) + \sum_{ij} \Phi(R_{ij}, V) \tag{3}$$

where the dominant term $f(V)$ depends on the volume only and includes the main part of the kinetic, exchange and correlation energy of the electron gas and of the electrostatic energy of the ion core in the electron gas. For a given pressure, it largely controls the resulting

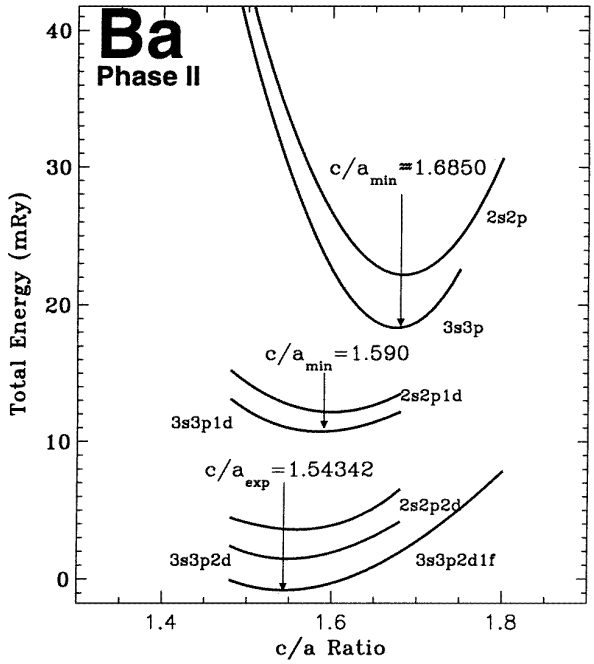

(a)

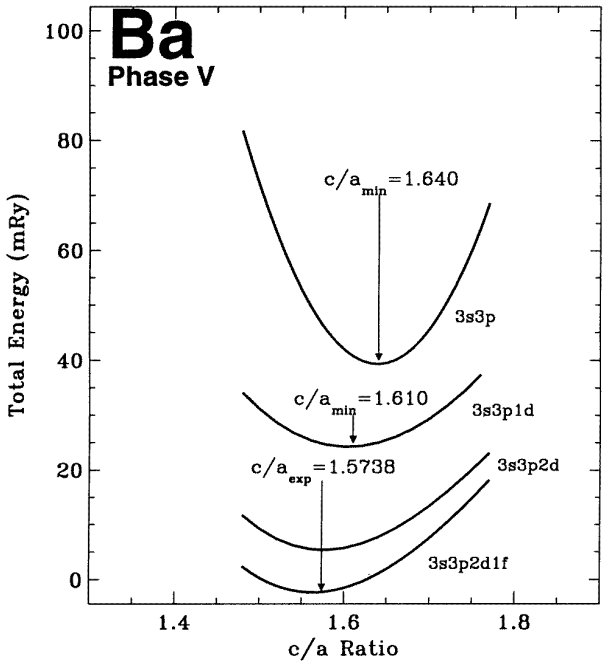

(b)

Figure 4. Total energy (relative) of barium in the hcp structure (a) in phase II at a volume corresponding to 7.21 GPa and (b) in phase V for 57.73 GPa as a function of the *c/a* ratio for different choices of the basis set. Each curve is displaced vertically by an arbitrary amount for clarity, labelled according to the notation explained in the text.

volume. $\Phi(R_{ij}, V)$ is a spherically symmetric pair potential between the ions, not strongly dependent on the volume V of the system [22, 42], so for brevity we shall not indicate the dependence on V explicitly hereafter. Note that $\Phi(R_{ij})$ is a rearrangement potential at a constant volume, with the volume largely fixed by the $f(V)$ term in equation (3), so the equilibrium nearest-neighbour distance between atomic centres does not necessarily lie at or near any minimum of $\Phi(R_{ij})$.

The theory of equation (3) is valid even for atoms containing d electrons as shown by Caroli [43] provided one adds an appropriate resonance term [36] to $\Phi(R_{ij})$. In this form the theory has been applied successfully to the alkaline-earth metals by various authors (see for example references [44–47]).

We now apply equation (3) to the variation of the total energy with *c/a* ratio. We consider the system at fixed volume V_{at} per atom

$$V_{at} = \frac{\sqrt{3}}{2}a^2c = Ca^3\gamma = Ca_0^3\gamma_0 \tag{4}$$

where γ is the *c/a* ratio and $\gamma_0 = \sqrt{8/3} \approx 1.632$, the ideal *c/a* ratio. Also C is a constant, a is the usual lattice constant and a_0 is the lattice constant for the ideal structure with the same atomic volume. The non-ideal structure has six near neighbours at a distance a in the close-packed plane perpendicular to the c-axis, and six near neighbours at a distance d, say, in the close-packed layers just above and below, corresponding to the twelve equidistant nearest neighbours in the ideal structure [48]. The total sum of pairwise interactions over the twelve near neighbours can therefore be written (per atom) as

$$\begin{aligned}\Phi_{tot} = \frac{1}{2}[6\Phi(a) + 6\Phi(d)] = 6\Phi(a_0) + {} & 3\left(\left.\frac{\partial\Phi}{\partial r}\right|_{r=a_0}(a-a_0) + \frac{1}{2}\left.\frac{\partial^2\Phi}{\partial r^2}\right|_{r=a_0}(a-a_0)^2\right. \\ & \left. + \frac{1}{3!}\left.\frac{\partial^3\Phi}{\partial r^3}\right|_{r=a_0}(a-a_0)^3 + \cdots\right) \\ & + 3\left(\left.\frac{\partial\Phi}{\partial r}\right|_{r=a_0}(d-a_0) + \frac{1}{2}\left.\frac{\partial^2\Phi}{\partial r^2}\right|_{r=a_0}(d-a_0)^2\right. \\ & \left. + \frac{1}{3!}\left.\frac{\partial^3\Phi}{\partial r^3}\right|_{r=a_0}(d-a_0)^3 + \cdots\right).\end{aligned} \tag{5}$$

It is convenient to define the deviation η from ideality by

$$\eta = \frac{\gamma}{\gamma_0} - 1 \tag{6}$$

and then the a, d can be expanded in terms of the η as follows:

$$\begin{aligned}a &= a_0\left(1 - \frac{1}{3}\eta + \frac{2}{9}\eta^2 - \frac{14}{81}\eta^3 + \cdots\right) \\ d &= a_0\left(1 + \frac{1}{3}\eta + \frac{1}{9}\eta^2 - \frac{11}{81}\eta^3 + \cdots\right).\end{aligned} \tag{7}$$

Substituting into equation (5) gives

$$\begin{aligned}\Delta\Phi_{tot}(\eta) &= \Phi_{tot} - \Phi_{tot}(\text{ideal}) \\ &= \left(\left.\frac{\partial\Phi}{\partial r}\right|_{r=a_0} + \frac{1}{3}a_0\left.\frac{\partial^2\Phi}{\partial r^2}\right|_{r=a_0}\right)a_0\eta^2 \\ &\quad + \left(\frac{25}{27}\left.\frac{\partial\Phi}{\partial r}\right|_{r=a_0} + \frac{1}{9}a_0\left.\frac{\partial^2\Phi}{\partial r^2}\right|_{r=a_0}\right)a_0\eta^3 + \cdots.\end{aligned} \tag{8}$$

As might be expected, the linear term in η cancels out, and the stability or otherwise of the ideal structure is largely determined by the sign of the second-order term. If it goes negative, then we expected the equilibrium *c/a* to deviate substantially from the ideal value [23, 24]. The third-order term determines whether the equilibrium will occur at *c/a* greater or less than the ideal value ($\sqrt{8/3}$).

We have taken $\Phi(R_{ij})$ for barium from the work of Jank and Hafner [36] which included both the sp and d electron contributions at one volume corresponding to ambient pressure. We have not recalculated $\Phi(R_{ij}, V)$ with smaller and larger proportions of d electrons, or at smaller volumes corresponding to high pressures, for several reasons. Firstly $\Phi(R_{ij}, V)$ in general does not depend strongly on volume [22, 42] although in the present case the variation in the proportion of d electrons will effect it. Secondly we are seeking here a semiquantitative understanding of the experimental results, not trying to reproduce the data accurately. Thirdly at the pressures considered here, there may be an appreciable additional interaction due to the $5p^6$ core shell. Fourthly in barium under pressure the proportion of d electrons has become so large that we are outside the proper range of validity of the theory: in fact there will be significant three-atom etc contributions from the d band. However, we believe that the theory with a fixed $\Phi(R_{ij})$ captures the dominant terms in the energy and suffices to give a correct interpretation of the experimental results.

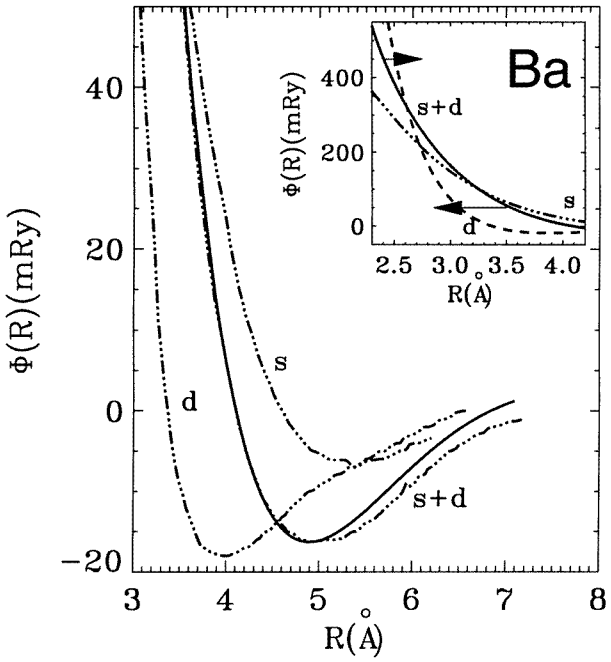

Figure 5. The pair potential of barium as a function of interatomic distance from reference [36] using hybridized pseudopotential tight-binding-bond theory, showing the separate contribution from the s and the d electrons, the total s + d and the fit of equation (9) to the s + d curve.

$\Phi(R)$ taken from reference [36] is shown in figure 5, and also shown broken down into separate s and d contributions. The nearly-free-electron tight-binding-bond approach assumed a band width of $W_d = 7.0$ eV and an average nearest-neighbour d–d hopping integral of $h(R_0) = 0.6217$ eV. A configuration of 1.25 s electrons and 0.75 d electrons

was assumed. $\Phi(R)$ has the customary form, a very repulsive screened pseudo-ion potential at short range, going over to Friedel oscillation at larger distance. The total $\Phi(R)$ from s and d electrons could be fitted quite well, especially in the region of 3 to 4 Å of interest here, by the form

$$\Phi(R) = C\frac{\cos(C_1 R)}{(C_1 R)^{\delta}} + \frac{B}{(R/R_0)^{12}} \tag{9}$$

with the parameter $C = -35.75$ Ryd, $C_1 = 1.15$ Å^{-1}, $\delta = 4.32$, $B = 1.90$ mRyd and $R_0 = 3.1$ Å. An analytic fit was necessary for the subsequent calculations.

It is clear from equation (8) that the instability of the ideal structure is driven by a cancellation between a negative first derivative Φ' and a positive second derivative Φ''. The negative part of the Friedel oscillation tends to cancel the positive tail of the hard-core repulsion, resulting in a very steep $\Phi(R)$ and large negative Φ' [42]. In our case the attractive part of the d-electron interaction has the same effect as seen in figure 5, making a large contribution in the range $R = 3.0$ to 3.5 Å. It is this steepness in $\Phi(R)$ which drives the instability, i.e. large negative Φ' in equation (8).

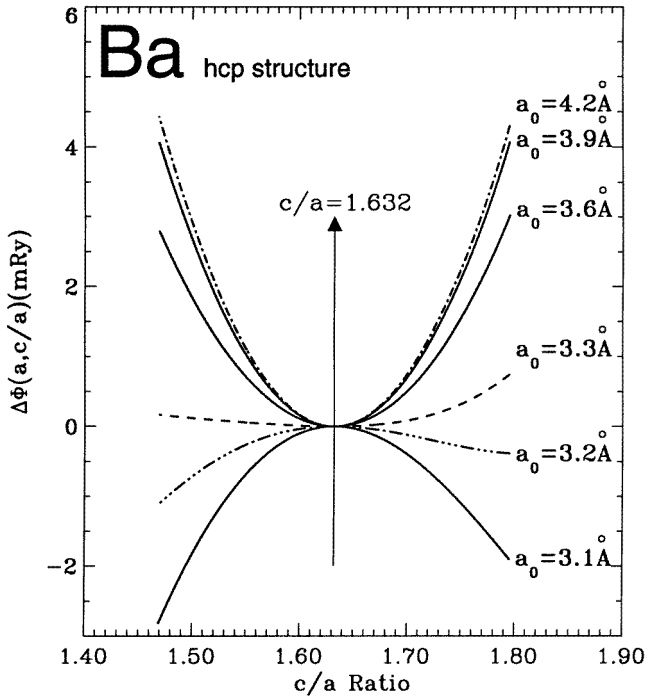

Figure 6. The pair potential contribution from the 12 nearest neighbours to the total energy of barium as a function of *c/a* at various fixed volumes (indicated by the respective a_0), relative to the ideal structure. The behaviour is similar to that observed in phase II, the ideal structure becoming unstable at lower volume.

Using the fitted $\Phi(R)$, we have evaluated Φ_{total} from the 12 nearest neighbours as a function of *c/a* at various fixed volumes (corresponding in figures 6 and 7 to fixed a_0 as defined by equation (4)). Figure 6 shows that an instability of the ideal structure does indeed set in with decreasing volume. This is taken to represent the experimentally observed situation in phase II. The calculated onset at $a_0 = 3.25$ Å does not correspond exactly to

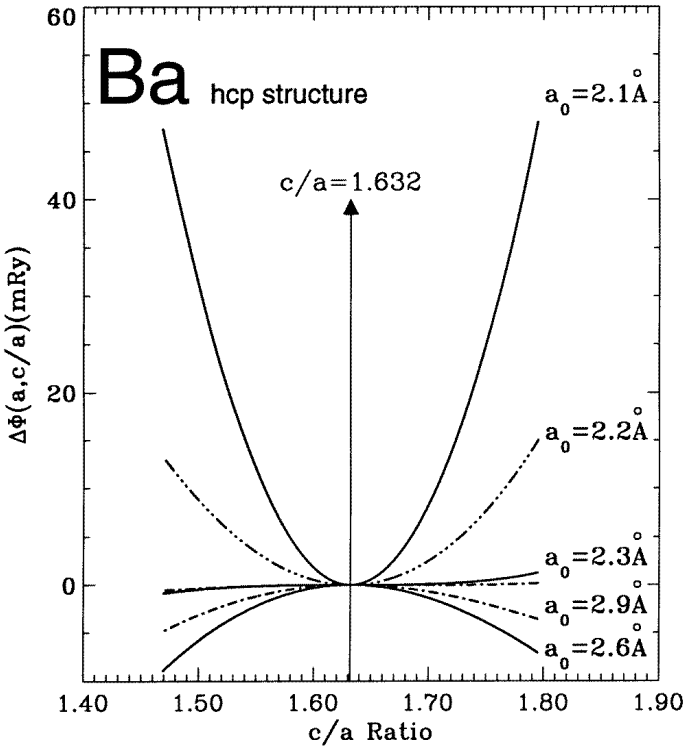

Figure 7. As figure 6, but for smaller volumes. The behaviour is that observed in phase V, the ideal structure becoming stable again. But when a_0 increases to 2.9 Å, the instability found in phase II will appear.

the observed onset at $a_0 \approx 4$ Å (figure 1 inset), but such a difference is only to be expected in view of the various approximations made. In fact the curves of the s and d components in figure 5 cross at $R = 2.6$ Å with the d component being very much the harder one. Thus the greater number of d electrons in barium under pressure (1.2 to 1.5, figure 2) compared with the number 0.75 assumed in reference [36], will move the onset of instability to larger values of a_0 as required by the data, as shown by the left-hand arrow in the inset of figure 5. The calculations were carried out with the expansion of equation (8) and not with $\Phi(R)$ directly, so no energy minimum is obtained at $a_0 < 3.25$ Å. However, the asymmetry of the curves shows clearly that the absolute minimum will lie at *c/a* less than the ideal value, as observed in barium.

Further similar total energy calculations at constant volume in the lower range of $a_0 = 2.1$ to 2.9 Å are shown in figure 7. On decreasing the volume, the instability now disappears, so the equilibrium structure again becomes close to the ideal packing. This corresponds to the observation in phase V. In the calculation, the reversion to ideal close packing occurs at $a_0 = 2.3$ Å, again too low a value compared with experiment for the same reason as before. Since there is no linear term in η in equation (8), the value of *c/a* will be exactly ideal once the system is out of the instability in our simple theory. In reality there is a small linear term from more distant neighbours and other higher-order terms in the theory, which are beyond the present calculations. A reversion to 'hard-sphere' behaviour and hence ideal packing is expected at very high pressure, because atoms become harder

and harder at small distance. It is easy to verify from equation (8) that a simple interaction

$$\Phi(R) \sim \exp(-R/\lambda) \tag{10}$$

gives the ideal structure as stable for λ less than $a_0/3$, i.e. less than 1 Å in our case. Even the Thomas–Fermi screening length from the conduction electrons is of the order of 0.5 Å, and the effect of the d electrons representing the cut-off of the atomic d-orbital function will be much sharper, as shown by the right-hand arrow in the inset of figure 5.

5. Conclusions

In conclusion, we have assembled various types of calculation to give an overall understanding of the observed behaviour of barium in the two hcp structures, phases II and V, under pressure. Firstly there is the electron transfer, mainly s to d as expected from previous works, but saturating and with some transfer into f orbitals at the highest pressures (50–100 GPa) in phase V. Fully self-consistent FP-LMTO total energy calculations have reproduced the observed behaviour of the *c/a* ratio quite well, and by dropping various orbitals from the basis set we have demonstrated that it is indeed the transfer into d orbitals that is driving the instability in *c/a* in phase II, and the fact that *c/a* is less than the ideal value in both phases II and V. Finally we have discussed the instability of the ideal structure in phase II and its re-establishment in phase V in terms of a simple pseudopotential perturbation theory, as modified by Hafner and other authors to take into account the influence of the d component in the electron states. This theory was taken over from a similar discussion relating to the behaviour of the *c/a* ratio in the series Be, Mg, Zn, Cd, and Hg [23, 24, 49] where there is an instability of the ideal close-packed structure similar to that in phase II of barium. Several approximations mean that the theory is only a semiquantitative interpretation of the experimental data. However, we expect the picture it presents to be valid, because experience with many such pseudopotential perturbation calculations has shown that they tend to be quite robust, i.e. not sensitive to detailed tuning of the pseudopotential [22, 50], with the second-order terms really being dominant [51]. The theory involves the pairwise interatomic rearrangement potential $\Phi(R_{ij}, V)$ at constant volume. The instability of the ideal structure is driven by Φ being very steep where a very repulsive screened ion interaction at short R goes over into an attractive outer region due to the d electrons and Friedel oscillations.

Acknowledgments

Useful discussions with A I Liechtenstein about the FP-LMTO program are gratefully acknowledged. W-S Zeng would like to acknowledge financial support by the Max-Planck-Gesellschaft during his stay at the Max-Planck-Institut für Festkörperforschung, Stuttgart, Germany. W-S Zeng is also grateful to O K Andersen for his considerable help and much encouragement. Interaction between Stuttgart and Cambridge was assisted by the HCM Network of the European Union: '*Ab initio* (from electronic structure) calculation of complex processes in materials' (contract No ERBCHRXCT 930369).

References

[1] Moriarty J A 1986 *Phys. Rev.* B **34** 6738
[2] Skriver H L 1982 *Phys. Rev. Lett.* **49** 1768
[3] Skriver H L 1985 *Phys. Rev.* B **31** 1909

[4] Moriarty J A 1986 *Phys. Rev.* B **34** 6738
[5] Takemura K 1994 *Phys. Rev.* B **50** 16 238
[6] Duthie J C and Pettifor D G 1977 *Phys. Rev. Lett.* **38** 564
[7] Porsch F and Holzapfel W B 1993 *Phys. Rev. Lett.* **70** 4087
[8] Hall H T, Merrill L and Barnett J D 1964 *Science* **146** 1297
[9] Glötzel D and McMahan A K 1979 *Phys. Rev.* B **20** 3210
[10] Boehler R and Ross M 1984 *Phys. Rev.* B **29** 3673
[11] Koskenmaki D C and Gschneidner K A 1978 *Handbook of the Physics and Chemistry of Rare Earths* vol 1, ed K A Gschneidner and L Eyring (Amsterdam: North-Holland) p 337
[12] Min B I, Jansen H J F, Oguchi T and Freeman A J 1986 *Phys. Rev.* B **34** 369
[13] Andersen O K 1975 *Phys. Rev.* B **12** 3060
[14] Jepsen O and Andersen O K 1995 *Z. Phys.* B **97** 35
[15] Methfessel M 1988 *Phys. Rev.* B **38** 1537
[16] Methfessel M, Rodriguez C O and Andersen O K 1989 *Phys. Rev.* B **40** 2009
[17] Moriarty J A 1977 *Phys. Rev.* B **16** 2537
Moriarty J A 1982 *Phys. Rev.* B **26** 1754
Moriarty J A 1988 *Phys. Rev.* B **38** 3199
[18] Wills J M and Harrison W A 1984 *Phys. Rev.* B **29** 5486
[19] Hausleitner C and Hafner J 1988 *J. Phys. F: Met. Phys.* **18** 1025
[20] Hausleitner C and Hafner J 1990 *Phys. Rev.* B **42** 5863
[21] Heine V and Weaire D 1966 *Phys. Rev.* **152** 603
[22] Hafner J and Heine V 1983 *J. Phys. F: Met. Phys.* **13** 2479
[23] Heine V and Weaire D 1970 *Solid State Physics* vol 24 (New York: Academic) p 249
See particularly pp 259–80 and 391–405.
[24] Weaire D 1968 *J. Phys. C: Solid State Phys.* **1** 210
[25] Heine V and Weaire D 1970 *Solid State Physics* vol 24 (New York: Academic) pp 418–27
See particularly p 420.
[26] Hohenberg P and Kohn W 1964 *Phys. Rev.* B **136** 864
[27] Kohn W and Sham L J 1965 *Phys. Rev.* A **140** 1135
[28] Andersen O K and Jepsen O 1984 *Phys. Rev. Lett.* **53** 2571
[29] Andersen O K, Jepsen O and Glötzel D 1985 *Highlights of Condensed-Matter Theory* ed F Bassani, F Fumi and M P Tosi (New York: North-Holland)
[30] Andersen O K, Jepsen O and Sob M 1987 *Electronic Band Structure and Its Application (Springer Lecture Notes in Physics)* ed M Yussouff (Berlin: Springer)
[31] Hedin L and Lundqvist B 1971 *J. Phys. C: Solid State Phys.* **4** 2064
[32] Jepsen O and Andersen O K 1971 *Solid State Commun.* **9** 1763
[33] Söderlind P, Ahuja R, Eriksson O, Johansson B and Wills J M 1994 *Phys. Rev.* B **49** 9365
[34] Ahuja R, Wills J M, Johansson B and Eriksson O 1993 *Phys. Rev.* B **48** 16 269
[35] Price D L and Cooper B R 1989 *Phys. Rev.* B **39** 4945
[36] Jank W and Hafner J 1990 *Phys. Rev.* B **42** 6926
[37] Mackintosh A R and Andersen O K 1980 *Electrons at the Fermi Surface* ed M Springford (Cambridge: Cambridge University Press)
[38] Andersen O K, Skriver H L, Nohl H and Johansson B 1973 *Pure Appl. Chem.* **52** 93
[39] Vasvari B, Animalu A O E and Heine V 1967 *Phys. Rev.* **154** 535
[40] Ross M and McMahan A K 1982 *Phys. Rev.* B **26** 4088
[41] Ahuja R, Eriksson O, Wills J M and Johansson B 1995 *Phys. Rev. Lett.* **75** 3475
[42] Hafner J and Heine V 1986 *J. Phys. F: Met. Phys.* **16** 1429
[43] Caroli B 1967 *J. Phys. Chem. Solids* **28** 1427
[44] Wills J M and Harrison W A 1983 *Phys. Rev.* B **28** 4363
[45] Harrison W A and Froyen S 1980 *Phys. Rev.* B **21** 3214
[46] Wills J M and Harrison W A 1984 *Phys. Rev.* B **29** 5486
[47] Moriarty J A 1988 *Phys. Lett.* **131A** 41
[48] Kittel C 1976 *Introduction to Solid State Physics* 5th edn (New York: Wiley)
[49] Hume-Rothery W and Raynor G V 1940 *Proc. R. Soc.* A **174** 471
[50] Hafner J 1987 *From Hamiltonians to Phase Diagrams (Springer Series in Solid State Science 70)* (Berlin: Springer)
[51] Heine V and Hafner J 1989 Volumes and pair forces in solids and liquids *Many-Atom Interactions in Solids* ed R M Nieminen *et al* (Berlin: Springer) pp 12–33